IOP Conference Series: Earth and Environmental Science

Draft Tube Vortex Rope Analysis of a Pump-turbine Unit under Different Operating Conditions

Draft Tube Vortex Rope Analysis of a Pump-turbine Unit under Different Operating Conditions

Qilian He[1], Xingxing Huang[2], Huili Bi[1], Mengqi Yang[3], Haixia Yang[3] and Zhengwei Wang[1*]

[1]State Key Laboratory of Hydroscience and Engineering & Department of Energy and Power Engineering, Tsinghua University, Beijing,100084 China
[2]InnoFuture GmbH, Binzstrasse 5, 8953, Zürich, Switzerland
[3]Branch Company of Maintenance & Test, CSG Power Generation co., LTD., Guangzhou 511400, China

E-mail: wzw@mail.tsinghua.edu.cn

February 2022

Abstract. Pumped-storage power stations which can be flexibly adjusted for power generation and energy storage, are widely constructed worldwide. Pumped-storage units work under different operating conditions according to the demand of the power grid, and vortex ropes in the draft tube will appear and show different shapes under the partial load conditions of the unit in generation mode. The unstable pressure pulsation caused by the eccentric vortex ropes inside the draft tube may cause the vibration of the unit during operation. So it is important to study the characteristics of draft tube vortex ropes for flow and vibration analysis. In this paper, a three-dimensional model of the unit is fully established, and the unsteady calculations of 60 %, 86.7%, and 100 % load conditions in turbine mode are carried out by numerical calculations to obtain the flow characteristics of the full flow field. The pressure and velocity distributions, shapes of vortex rope in the draft tube under different load conditions are extracted from the CFD analyses, respectively. The pressure pulsations of different monitoring points set up inside the draft tube are evaluated in the time domain and frequency domain. The results show that the vortex rope in the draft tube is more obvious under small flow discharge, and the vortex rope itself is not sensitive to the selection of Q criterion threshold, but the vortex on the draft tube wall is greatly affected by the selection of the threshold. The influence of draft tube vortex ropes on the vibration of the pumped-storage unit is also discussed.

1. Introduction

Hydropower is widely used around the world because of its excellent cleanliness and flexibility. Pumped-storage power plants are gaining more and more attention as an important form of hydroelectric power generation and energy storage due to their advantages in choosing the direction of energy conversion. The safe operation of the unit is the main concern of every power station. Draft tube vortex rope may cause unstable flow and abnormal pressure pulsation of units, further cause abnormal structural vibration and threaten the operation safety of units. Pumped-storage units often work under conditions deviating from the optimum conditions according to the demand of the power grid. Especially under partial load operating conditions, the draft tube vortex rope phenomenon is more significant. Unstable pressure fluctuation caused by the draft tube vortex rope phenomenon may lead to structural fatigue failure of units. Therefore, it is very important to study the characteristics of draft tube vortex ropes for flow and vibration analysis and the safe operation of the power station.

There have been a number of studies on the eccentric vortex rope of the draft tube. Some studies[1, 2, 3, 4] believe that the low-frequency pressure pulsation of the draft tube is caused by vortex rope underrated working conditions or low flow conditions, and these low-frequency pressure pulsations are the main reason affecting the normal operation of the unit[5, 6]. The numerical simulation method is the most popular research method of unit flow and pressure pulsation. Some studies[7, 8, 9] compared the differences between numerical calculation and experimental measurement results and proved the reliability and accuracy of the calculation results of the numerical simulation method. However, for the full three-dimensional modeling and simulation of Pumped-storage units, the research on draft tube vortex is still insufficient, which needs in-depth research.

In this paper, the full three-dimensional flow channel model of a pumped-storage unit was established, including volute, stay vane, guide vane, runner, draft tube, balance tubes, upper labyrinth seal, and lower labyrinth seal. The unsteady flows of the unit under 60%, 86.7%, and 100% load in generation mode were calculated, and the investigated vortex ropes of draft tubes with different shapes were analyzed. The results show that the vortex rope is more obvious under a lower load, and the pressure fluctuation of the draft tube is more intense.

2. Calculation methods

The differential form of Navier-Stokes equations describing fluid motion is:

$$\frac{\partial \rho}{\partial t}+\frac{\partial}{\partial x_i}\left(\rho u_i\right)=0 \tag{1}$$

$$\frac{\partial}{\partial t}\rho u_i+\frac{\partial}{\partial x_j}(\rho u_i u_j)=\frac{\partial \tau_{ij}}{\partial x_j}+\rho f_i \tag{2}$$

The Reynolds time-averaged method is used for treatment, and the Reynolds stress is defined as

$$\tau_{ij}=-\rho\overline{u'_i u'_j} \tag{3}$$

The continuity equation and momentum equation can be expressed as:

$$\frac{\partial \rho}{\partial t}+\frac{\partial}{\partial x_j}\left(\rho u_j\right)=0 \tag{4}$$

$$\frac{\partial}{\partial t}(\rho u_i) + \frac{\partial}{\partial x_j}(\rho u_i u_j) = -\frac{\partial p}{\partial x_i} + \frac{\partial}{\partial x_j}\left(\mu \frac{\partial u_i}{\partial t} + \tau_{ij}\right) + S_M \tag{5}$$

where the overline is omitted, ρ is the density, p is the pressure, i and j are indicators which fall in $1, 2, 3$, u_i is the velocity component in x, y and z directions, μ is the dynamic viscosity, S_M is the generalized source term of the momentum conservation equation.

In this paper, SST $k-\omega$ model is used as the correction of the eddy viscosity model. Compared with $k-\epsilon$ model and standard $k-\omega$ model, SST $k-\omega$ model combines the advantages of both by using different models flexibly in the near-wall region and free turbulence region. SST $k-\omega$ model is widely used in hydraulic machinery calculation and has been proved to be a robust and effective method.

3. Calculation models and meshes

3.1. Computational fluid domain model and boundary conditions

The fluid domain model of the unit is composed of volute, stay vane, guide vane, runner, draft tube, balance tubes, upper labyrinth seal, and lower labyrinth seal, as shown in Figure 1. The basic parameters of the unit are shown in Table 1. The calculation conditions include 100% load, 86.7% load, and 60% load, which are achieved by adjusting the opening of the guide vane. The calculation mode was set as transient, the interfaces type between the runner and other fluid domains were set as transient rotor-stator, and the other interfaces were set to None in General Connection. The total calculation time was 0.6 s and each step was 0.0006 s. The boundary conditions of the volute and the draft tube were set as pressure inlet and pressure outlet, respectively. The rotational speed of the runner fluid field were set as rated speed 500 rpm.

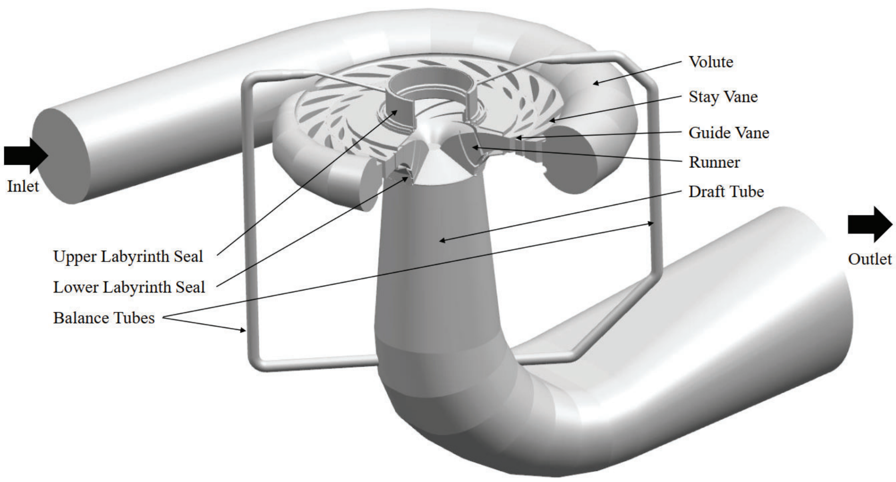

Figure 1. Computational fluid domain model of the unit.

Table 1. Unit Parameters.

Parameters	Uints	Values
Rated powerP_r	MW	300
Rated speed N_r	rpm	500
Rated head H_r	m	510
Runner blade number Z_r		7

The hybrid meshes with tetrahedra and hexahedra elements were built up for each flow passage of the unit. A hexahedral mesh with good computational quality was used to mesh the flow field with good structural topology, and a tetrahedral mesh with good adaptability is used to mesh the complex flow field. The mesh of the boundary layer near the wall was refined to ensure calculation accuracy. A multi-layer mesh was created to divide the labyrinth seals and the smaller overflow gaps such as the balancing pipe to ensure the accuracy of flow calculation.

The mesh of the straight cone section of the draft tube is additionally refined. The results of meshing are shown in Figure 2.

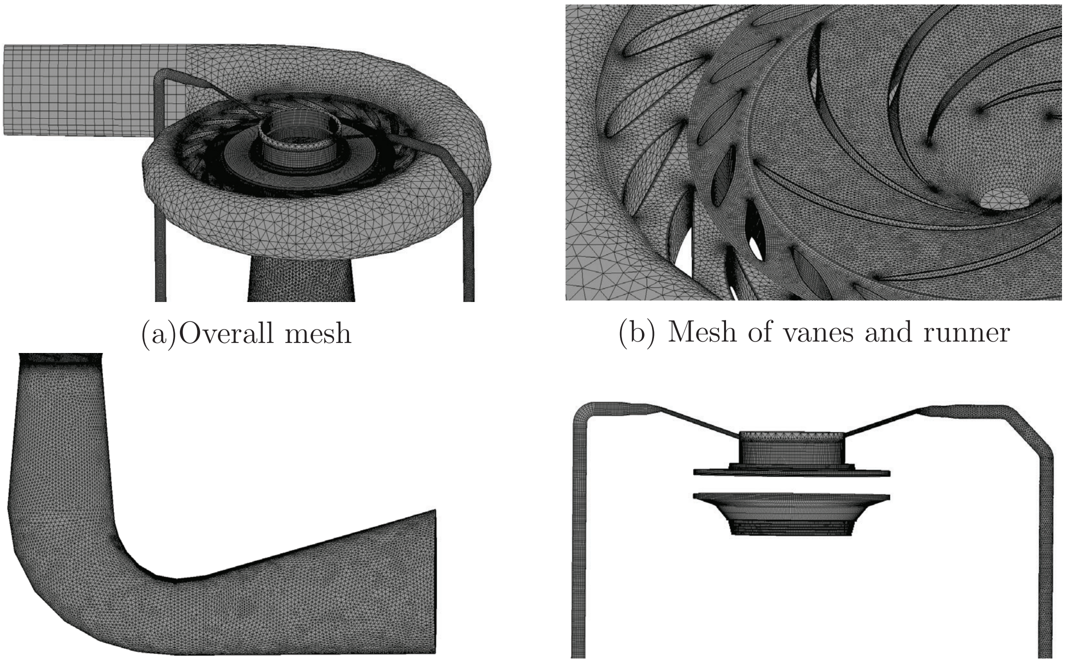

(a)Overall mesh (b) Mesh of vanes and runner

(c) Mesh of Draft tube (d) Mesh of labyrinth seal and balance tubes

Figure 2. Fluid domain mesh of the unit.

Three sets of computational mesh (7 million, 8.5 million, and 10 million) are used to verify the mesh independence. When the number of mesh is greater than 8.5million, the error of efficiency calculation results of each set of meshes does not exceed 3%. Therefore, the unsteady calculation is carried out by using 8.5million (including 2.5million draft tube mesh) as a whole.

4. Results of Calculation

4.1. Vortex rope distribution of draft tube under different load conditions

The Q criterion is used to identify the vortex zone of the draft tube, and the Q value is set to 500 s^{-2}. The streamline and vortex zone of the draft tube under different loads is shown in figure 4.

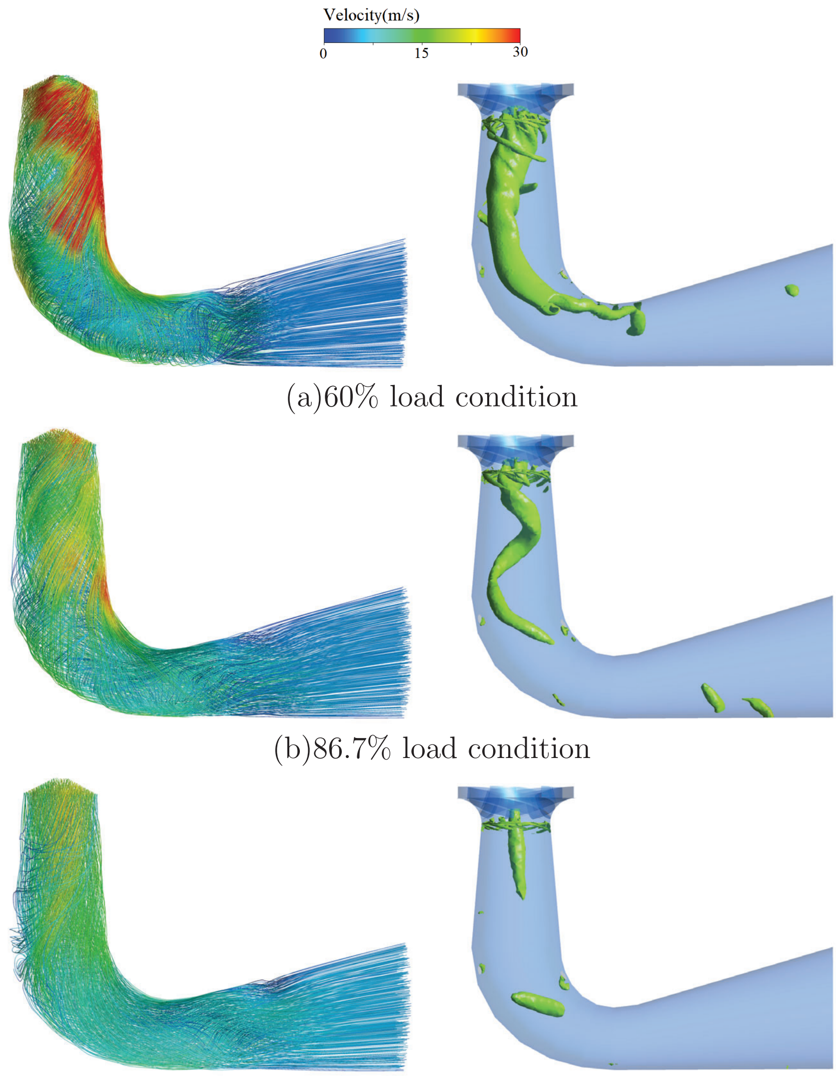

(a)60% load condition

(b)86.7% load condition

(c)100% load condition

Figure 3. Draft tube vortex rope under three operating conditions.

There are three types of vortex in the draft tube: eccentric rotating draft tube vortex rope starting downstream of the runner center, residual continuation of some of the eddy ducts starting from the flow channel between the runner blades, and annular fine vortex entering the draft tube from the lower labyrinth seal. The draft tube vortex rope is straight columnar when the unit operates at 100% load and disappears quickly upstream of the straight cone section. When the unit operates under 86.7% load, the draft tube vortex rope presents a slender rotating shape. When the unit operates at 60% load, the draft tube vortex rope is strong and its diameter is about twice that of the vortex rope under other operating conditions. And the vortex rope extends to the draft tube diffusion section. Under 60% condition, the flow in the draft tube is very disordered, and the strength of other vortices such as the extended vortices in the runner blade channel increases. The cause of vortex rope can be explained by flow theory. When the unit works at the optimum operating point, the flow at the runner outlet follows the normal direction without forming a speed loop. When the actual flow rate of the unit is less than the designed flow rate, the absolute speed at the outlet of the runner has a component in the direction of rotation of the runner, thus generating a positive circulation, which causes the circumferential velocity of the water flow after it enters the draft tube. The lower the flow rate, the larger the velocity loop at the runner outlet and the stronger the vortices in the draft tube center.

The eccentricity of the draft tube vortex rope results from the asymmetry of the unit, and the uneven circumference between the volute and guide vane results in an eccentric resultant force on the flow at the runner outlet. This explains the appearance of eccentric rotating draft tube vortex rope in the unit.

4.2. Flow characteristics analysis in draft tube

Four cross-sections at different positions in the straight cone section of the draft tube are cut out(an additional cross-section in the elbow section for low load conditions). Define the pressure coefficient $C_p = p/\rho g H_r$, where ρ is the density of water, g is the gravity acceleration, H_r is the head.

The interface pressure and velocity contours are shown in Figure 4. Local pressure valleys and local vorticity peaks occur at the locations through which the draft tube vortices pass. Under low load conditions, the draft tube inlet section receives the influence of vortex shedding in the runner blade channels, and more high vorticity areas appear in the draft tube main vorticity except in the vorticity contours. The pressure contour shows that the lower the load, the larger the low-pressure area and the lower the absolute pressure.

This is consistent with the mechanism of vortex rope formation. Low flow leads to larger circulation and stronger vortices so that the range of vortices is enlarged, the central pressure is reduced, and the pressure drop extends to the draft tube diffusion section along with the vortices. The characteristics of the vorticity intensity contours are similar. In the draft tube inlet section, a strong vorticity area surrounding the avoidance occurs due to the shedding of the runner blade duct vortices, which disappear faster than the main vortex in the draft tube.

The longitudinal section streamline of the draft tube is shown in Figure 5. Under 60% load condition, the eddy current extends from the straight cone section to the diffusion section, and the eddy current phenomenon is very obvious. Under 86.7% load condition, the vortex is concentrated in the straight cone section, the interface appears

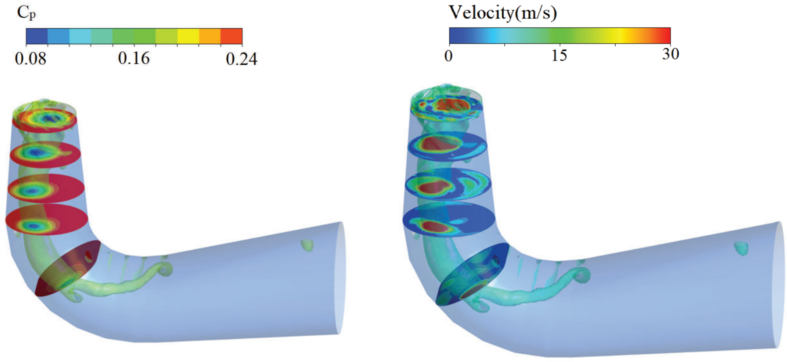

(a)60% load condition

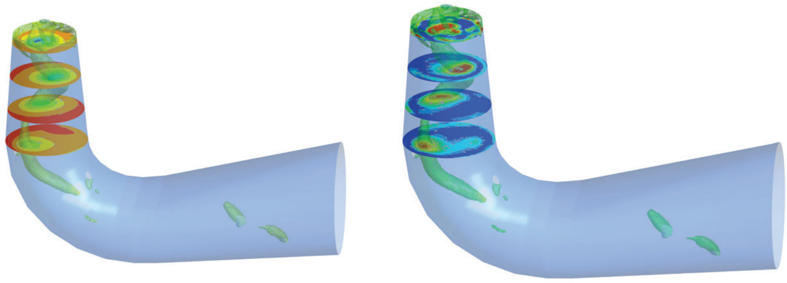

(b)86.7% load condition

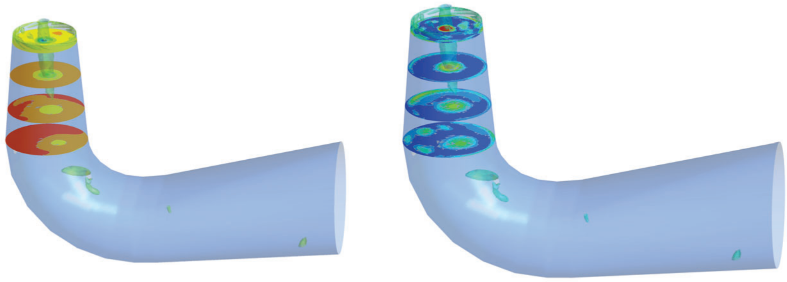

(c)100% load condition

Figure 4. Pressure and Vorticity contour at different cross-sections in the draft tube.

asymmetric vortex, and the eccentricity between the vortex zone and the draft tube is mild. Under 100% load condition, the inlet velocity of the draft tube is normal, there is almost no inlet circulation, and there is no obvious vortex rope in the longitudinal section.

4.3. Pressure fluctuation analysis of draft tube monitoring points

A CFX pressure monitoring point is set in the straight cone section of the draft tube, which is close to the pipe wall and is in the same position as the actual measured sensor, as shown in Figure 6. Define $f_n = 8.33$ Hz is the runner passing frequency(The speed is 500 rpm and the number of runner blade is 7). The time-domain and frequency-domain diagrams of draft tube measuring points under different conditions are shown in Figure 7. The pressure coefficient is still defined as $C_p = p/\rho g H_r * 100\%$,which represents the proportion of pressure pulsation to head.

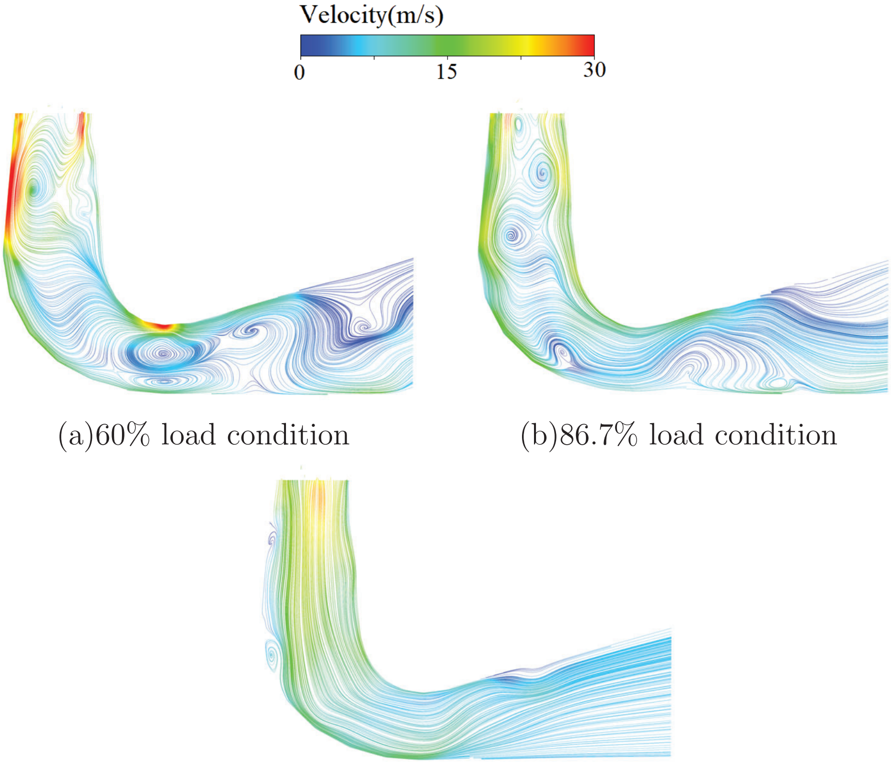

(a)60% load condition (b)86.7% load condition

(c)100% load condition

Figure 5. Streamline at the longitudinal section of the draft tube.

The low frequency signal amplitude of draft tube measuring point reaches 0.59% under 60% load, 0.3% under 86.7% load and less than 0.15% under 86.7% load. The law of pressure ripple in draft tube is obvious. The lower the load, the lower the flow rate and the greater the amplitude of low-frequency pressure ripple. Meanwhile, the low frequency signal is more abundant under the low flow condition, and has an amplitude in the frequency of about 1-3 times rotation frequency, while only 1 times rotation frequency shows a single peak under the 100% load condition. The hydraulic excitation from the static and dynamic interference is greatly weakened by the runner, which shows a peak value at 21 times frequency in the draft tube, with an amplitude of 0.15%, much smaller than that of 21 times frequency in the vaneless area.

As the amplitude of draft tube measuring point under 100% load condition is very small, the measured error will be magnified, which makes the error analysis meaningless. Therefore, only 86.7% and 100% load condition calculation results are compared with the field measured results.

The amplitude of low frequency signal under 60% load condition and 86.7%load condition is compared with the field measured amplitude. The comparison results are shown in figure 8 and table 2. Due to the error of the two equation model, the details such as welding chamfer are not considered in the modeling, and the measurement is affected by the accuracy of instruments and human factors, the error is acceptable.

doi:10.1088/1755-1315/1079/1/012012

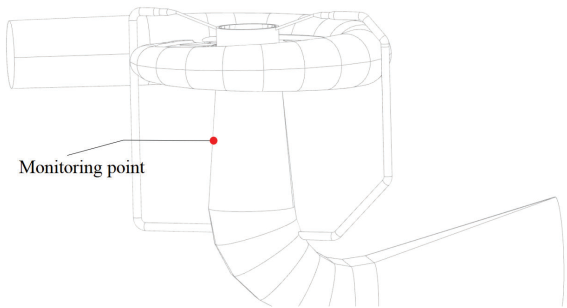

Figure 6. pressure monitoring point

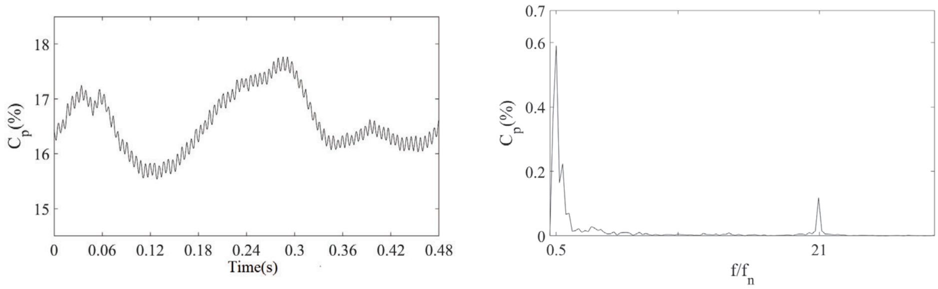

(a)60% load condition

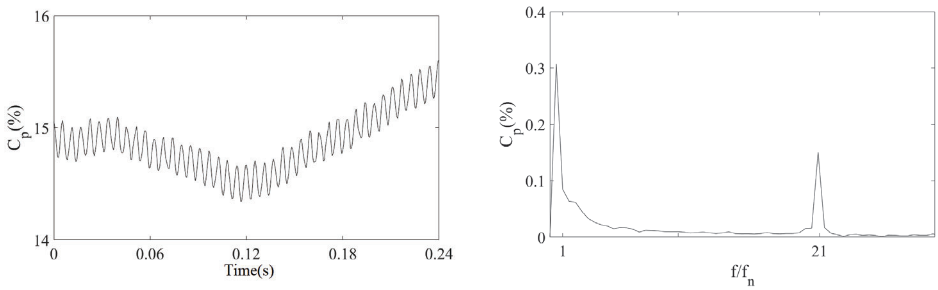

(b)86.7% load condition

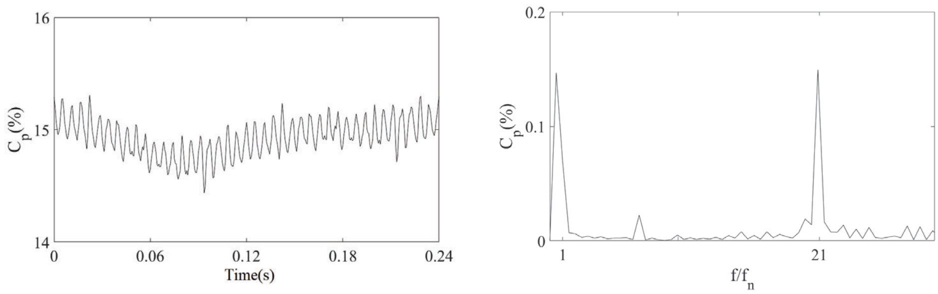

(c)100% load condition

Figure 7. Time-domain and frequency-domain diagrams of pressure fluctuation at draft tube.

5. Conclusion

In this paper, a prototype pump turbine under different load conditions is simulated, the flow characteristics and vortex rope phenomenon in the draft tube are analyzed in detail,

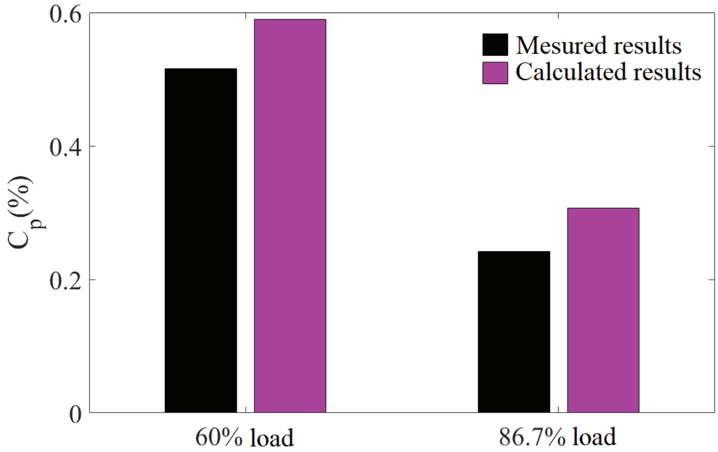

Figure 8. Comparisons between calculation of low-frequency pressure amplitude and measured results

Table 2. Unit Parameters.

Conditions	measured results($C_p/\%$)	calculated results($C_p/\%$)	error(%)
60% load	0.516	0.590	12.5
86.7% load	0.242	0.307	21.2

and compared with the measured results to verify the effectiveness of the calculation. The calculation results show that there is an obvious phenomenon of draft tube vortex rope in the unit under low flow conditions. The draft tube vortex rope becomes stronger with the decrease of flow.

Under 60% load condition, the draft tube vortex rope is thick and extending to the diffusion section, a large number of high-speed wall swirls appear, and low-pressure and high-speed flow areas appear in the center of the vortex rope. Under the condition of 86.7% load, the vortex rope is rotating, disappears at the end of the straight cone section of the draft tube, and the vortex rope strength becomes weak. Under 100% load, the vortex is short and eccentric.

The pressure pulsation of draft tube is enriched with low-frequency signals, and the pressure peak is shown in low-frequency under all working conditions. The peak value of low-frequency pressure increases with the decrease of flow rate. The influence of Rotor-Stator Interaction still propagates to the draft tube to a certain extent, resulting in a peak at 21 times the frequency in the frequency domain diagram.

In this paper, the flow and pressure characteristics of draft tube are obtained, and the results can be used as the boundary conditions of fluid-structure coupling calculation to continue the dynamic characteristics analysis of unit structural components.

Acknowledgments

Authors would like to acknowledge the financial support of the project: *Research on Lifetime Prediction of Non-rotating Parts of Pump Turbine Unit Based on Rotor-Stator Interaction (RSI), Fluid-Structure Coupling and Fracture Mechanics—Research project on RSI mechanism and its Influence on Non-rotating parts of Pump Turbine Unit* of Branch Company of Maintenance & Test, CSG Power Generation co., LTD.

References

[1] Wack J and Riedelbauch S 2017 *Journal of Physics: Conference Series* **813** 012019
[2] Susan-Resiga R, Muntean S, Stein P and Avellan F 2009 *International Journal of Fluid Machinery and Systems* **2** 295–302
[3] Iliescu M, Ciocan G and Avellan F 2008 *Journal of Fluids Engineering* **130** 146–157
[4] Zhu L, Meng X C, Zhang J G, Chen Y, Zhang H P, Wang W and Lu L 2019 *IOP Conference Series Earth and Environmental Science* **240**
[5] Zheng Y, Jiang W, Chen Y and Sun A 2018 *Transactions of the Chinese Society for Agricultural Machinery*
[6] Chen T, Zheng X, Zhang Y N and Li S 2018 *Journal of Hydrodynamics* **30** 131–139
[7] Mousmoulis G, Kassanos I, Anagnostopoulos J and Papantonis D 2015 Experimental and numerical investigation of the cavitating draft tube vortex in a francis model turbine *6th IAHR International Meeting of the Workgroup on Cavitation and Dynamic Problems in Hydraulic Machinery and Systems*
[8] Su W T, Li X B, Xu Y N, Gong R Z, Maxime B and Muhirwa A 2018 *Thermal Science* **22** 40–40
[9] Kc A, Lee Y H and Thapa B 2016 *Renewable Energy* **86** 1406–1421